

# Synchronization Line Defects in Oscillatory and Excitable Media

Andrei Goryachev and Raymond Kapral

*Chemical Physics Theory Group, Department of Chemistry, University of Toronto,  
Toronto, ON M5S 3H6, Canada*

**Abstract.** When the dynamics of a spatially distributed excitable or oscillatory medium is complex, synchronization defect lines may exist which lead to a variety of pattern formation processes. If a medium with period- $n$  local dynamics supports spiral waves, such synchronization defect lines are necessary to reconcile the fact that  $n$  rotations of a spiral wave are needed to restore the entire concentration field to its initial value. We show how such synchronization defect lines may be classified and how they can lead to line-defect turbulent states through non-equilibrium phase transitions.

## I INTRODUCTION

Complex periodic or chaotic oscillations do not have simple trajectories in concentration phase space. For example, a period- $n$  oscillatory motion is described by a period- $n$  orbit that loops  $n$  times in concentration phase space before closing on itself. In such circumstances no simple single-valued angle variable may be introduced to play the role of the phase. However, it is often possible to generalize the definition of phase even for systems whose dynamics is chaotic [1]. One may then discuss phase synchronization in complex periodic or chaotic media and the consequences of such synchronization for pattern formation.

One of the most visible consequences of phase synchronization in media with complex local dynamics is the existence of spiral waves. Computer simulations have demonstrated that spiral waves persist even if the local dynamics is chaotic [2–4]. If the underlying local dynamics has a phase space structure more complex than a simple closed loop, we show that spiral waves must be accompanied by line defects where the phase of the oscillation changes suddenly by multiples of  $2\pi$  [4,5]. These line defects change the structure and symmetry of spiral waves and in general influence the nature of spatio-temporal dynamics in these media. The line defects themselves may have distinctive dynamics and give rise to turbulent regimes characterized by the birth and destruction of line defects analogous to defect-mediated turbulence in oscillatory media [6].

CP501, *Stochastic Dynamics and Pattern Formation in Biological and Complex Systems*,  
edited by S. Kim, K. J. Lee, and W. Sung  
© 2000 American Institute of Physics 1-56396-914-9/00/\$17.00

In this paper we present an overview of these phenomena. We begin with a discussion of the concept of phase in complex oscillatory media. We then show how the nature of a spiral wave changes when simple oscillatory dynamics bifurcates to period-doubled or more complex oscillatory patterns. We show how the possible kinds of line defect may be deduced from a knowledge of a braid representation of the local orbits. Turbulent states arise when the system parameters are tuned to lie closer to the chaotic regime.

The phenomena described in this paper are general and should exist in a variety of complex periodic and excitable media. They have been recently observed in experiments on the Belousov-Zhabotinsky reaction by Park and Lee [7] and Yoneyama et al [8]. and their further investigation should lead to new mechanisms for pattern formation in reaction-diffusion systems.

## II PHASE OF COMPLEX OSCILLATIONS

As an example of a complex periodic oscillation consider the period-2 orbit in a three-dimensional concentration phase space  $(c_x, c_y, c_z)$  shown in Fig. 1. One can see from this figure that an angle variable  $\varphi$  may be defined in a cylindrical coordinate system but it does not uniquely parameterize points on the trajectory. For example, points  $A$  and  $A'$  on the orbit have the same value of  $\varphi$  but do not correspond to the same phase space point. Nevertheless, the phase variable  $\phi$  may be defined in terms of the angle variable  $\varphi$  as  $\phi = \varphi + 2\pi m$  where  $m$  is an integer with values 0 or 1 that distinguishes points on the orbit with identical  $\varphi$ . In the

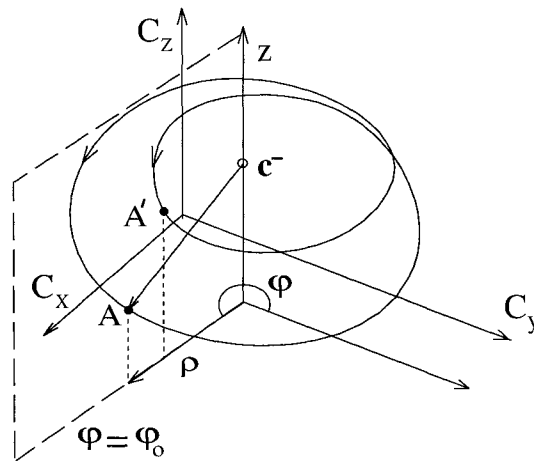


**FIGURE 1.** A period-2 orbit in the  $(c_x, c_y, c_z)$  concentration phase space. The two points  $A$  and  $A'$  lying in the semiplane  $\varphi = \varphi_0$  have phases  $\phi_A = \varphi_0$  and  $\phi_{A'} = \varphi_0 + 2\pi$  which differ by  $2\pi$ .

more general case for an orbit with period  $n$  the integer  $m$  ranges from 0 to  $n - 1$ . We may write  $\phi(t)$  more explicitly for a period- $n$  orbit as

$$\phi(t) = \phi(0) + \frac{2\pi n}{T_n}t + \psi(t) - \psi(0), \quad (1)$$

where  $\psi(t)$  is a  $T_n$ -periodic function with zero average value. Consider two oscillations  $\phi(t)$  and  $\phi'(t)$  with period  $T_n$  following the same orbit in phase space but time shifted by  $\delta t$ :  $\phi'(t) = \phi(t - \delta t)$ . Then

$$\delta\phi(t) = \phi(t) - \phi'(t) = \frac{2\pi n}{T_n}\delta t + \psi(t) - \psi(t - \delta t). \quad (2)$$

Averaging this difference over a period  $T_n$  we find

$$\overline{\delta\phi(t)} = \frac{1}{T_n} \int_0^{T_n} dt [\phi(t) - \phi'(t)] = \frac{2\pi n}{T_n}\delta t. \quad (3)$$

From this discussion one can see that  $\delta\Phi = \frac{2\pi n}{T_n}\delta t$  does not depend on time and measures the delay of one oscillation relative to the other in units of the full period phase increment  $2\pi n$ . From the definition of  $\delta\Phi$  it follows that this quantity is additive: consider three oscillations where the first and second differ by a time translation  $\delta_{12}t$  and the second and third by  $\delta_{23}t$ . Then  $\delta_{13}\Phi = \delta_{12}\Phi + \delta_{23}\Phi$ .

### III SPIRAL WAVES AND $\Omega$ LINES

Imagine a spiral wave in a simple oscillatory (period-1) medium and suppose a control parameter is changed and the local dynamics signals a bifurcation from period 1 to period 2. At such a bifurcation point the period of the orbit doubles so that  $T_2 \approx 2T_1$ . In the period-1 regime the spiral wave is assumed to have rotational symmetry such that evolution in time  $T_1$  corresponds to rotation through  $2\pi$  of the entire concentration field of the spiral about its center. Just beyond the bifurcation point where the period of the orbit doubles one full rotation of the spiral no longer restores the concentration field to its original value. Instead two spiral rotations are required to do this and rotational symmetry is broken.

To understand the nature of the broken rotational symmetry consider a closed path surrounding the spiral core. For a period-1 oscillation the phase variable is just the angle variable  $\varphi$  and the line integral of the gradient of the phase along the closed curve gives the topological charge  $\pm n_t$  of the spiral [9]:

$$\oint \nabla\varphi(\mathbf{r}, t) \cdot d\mathbf{l} = \pm 2\pi n_t. \quad (4)$$

For a stable one armed spiral  $n_t = 1$  [10] and one sees that the phase is incremented by  $2\pi$  along such a closed curve. Next, consider period-2 dynamics. The reaction-diffusion medium is continuous in space so that when the closed path surrounding

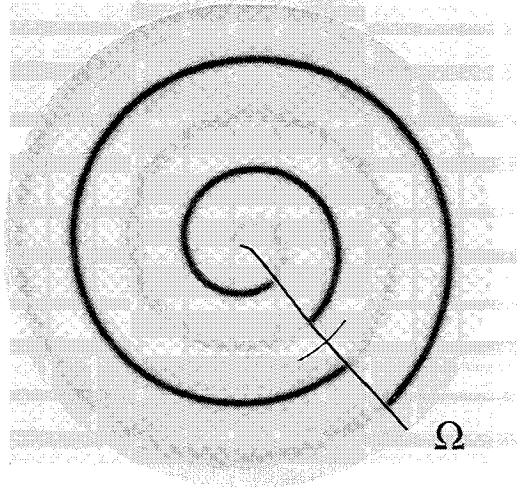


**FIGURE 2.** Spiral wave with period-2 local dynamics for the Rössler model with  $C = 3.84$ ,  $A = B = 0.2$  in a disk-shaped domain with radius  $r = 256$ . The  $c_z(\mathbf{r}, t)$  concentration field is shown in grey shades;  $\Omega$  curve at polar angle  $\theta_\Omega$  (solid line).

the defect is traversed one must arrive at the starting value of the concentration. In view of the fact that it takes two rotations of the spiral through an angle  $2\pi$  to restore the entire concentration field to its initial value, there must be an additional phase jump of  $2\pi$  to satisfy the continuity requirements. This phase jump of  $2\pi$  occurs along a line emanating from the spiral core. We term such a synchronization line defect an  $\Omega$  line.

The nature of the synchronization line defect is seen in Fig. 2 which plots the  $c_z(\mathbf{r}, t)$  concentration field at a single time instant for the Rössler reaction-diffusion system [11],

$$\begin{aligned}
 \frac{\partial c_x(\mathbf{r}, t)}{\partial t} &= -c_y - c_z + D\nabla^2 c_x \\
 \frac{\partial c_y(\mathbf{r}, t)}{\partial t} &= c_x + Ac_y + D\nabla^2 c_y \\
 \frac{\partial c_z(\mathbf{r}, t)}{\partial t} &= c_x c_z - Cc_z + B + D\nabla^2 c_z .
 \end{aligned} \tag{5}$$

There is an alternation of large and small amplitude segments in the spiral that arises from the period doubling of the simple oscillation. Along the  $\Omega$  line (drawn as a heavy solid line in the figure) one sees a sharp change from high to low concentration maxima corresponding to a  $2\pi$  jump in the phase of the oscillation. This jump in phase is clearly seen by examining the concentration time series on either side of the  $\Omega$  curve shown in Fig. 3. The time series at two points on opposite sides

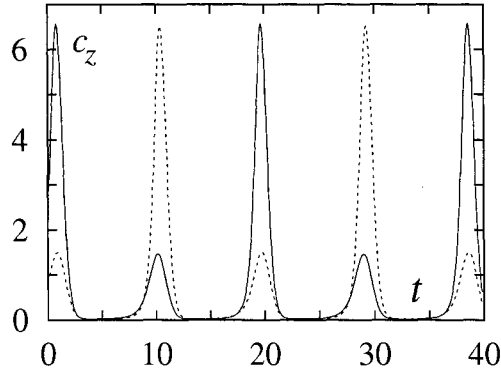


**FIGURE 3.** The  $c_z(t)$  concentration time series calculated at points  $\mathbf{r}_{1,2} = (r_0 = 130, \theta = \theta_\Omega \pm 0.05)$  on opposite sides of the  $\Omega$  curve.

of the  $\Omega$  curve on the thin solid line in Fig. 2 are identical in character but shifted relative to each other by half of a full period ( $2\pi$ ).

We may introduce a local phase variable  $\phi(\mathbf{r})$  to understand the structure of a medium with synchronization defect lines. Considering the dynamics at spatial point  $\mathbf{r}$  we may write  $\phi(\mathbf{r}, t) = \varphi(\mathbf{r}, t) + 2\pi m(\mathbf{r}, t)$  where  $m$  is an integer function. The line integral of the gradient of this phase along a closed path surrounding the spiral core must equal  $2\pi nk$ , a multiple of a full period of a period- $n$  oscillation. Consequently,

$$\begin{aligned} \oint \nabla \phi(\mathbf{r}, t) \cdot d\mathbf{l} &= \oint \nabla \varphi(\mathbf{r}, t) \cdot d\mathbf{l} + 2\pi \oint \nabla m(\mathbf{r}, t) \cdot d\mathbf{l} \\ &= \pm 2\pi + 2\pi \oint \nabla m(\mathbf{r}, t) \cdot d\mathbf{l}. \end{aligned} \quad (6)$$

In writing the second line of this equation we used the fact that for a one-armed spiral with topological charge  $n_t = \pm 1$  the line integral yields  $\pm 2\pi$  regardless of the periodicity of the local dynamics. Given that the full-period phase increment is  $2\pi$  only in the case of period-1 dynamics where  $m(\mathbf{r}, t) \equiv 0$ , for period- $n$  dynamics the second line integral will contribute. Since  $m(\mathbf{r}, t)$  is an integer function, its value changes discontinuously with time and space. The loci of these discontinuities can be identified with synchronization line defects.

It is interesting to consider the structure and transformations of local trajectories in phase space as the  $\Omega$  line is crossed. Once again we consider the moving along the arc in Fig. 2 that crosses the  $\Omega$  curve. The orbits at five points along this arc are shown in Fig. 4. As one traverses the arc, the larger, outer loop of the local orbit constantly shrinks while the smaller, inner loop grows. At  $\theta = \theta_\Omega$ , both loops merge and then pass each other exchanging their positions in phase space. (Compare left and right panels of Fig. 4.) As one sees from Fig. 4, at the exchange

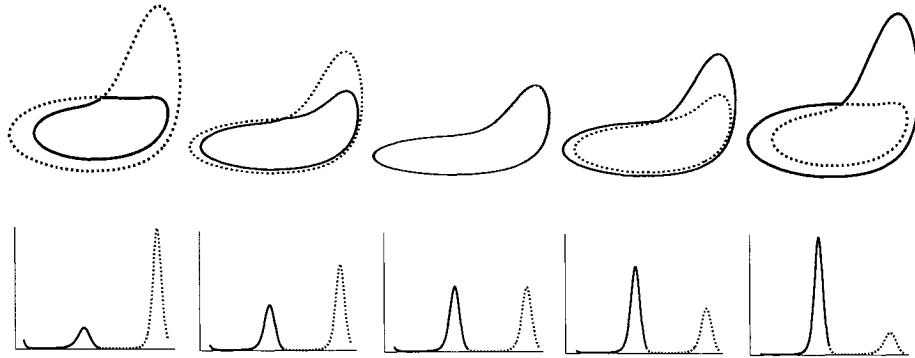


**FIGURE 4.** Loop exchange in local orbits in  $(c_x, c_y, c_z)$  phase space as the  $\Omega$  curve is crossed. First and second halves of an oscillation period are shown by different styles of line.

point  $\theta = \theta_\Omega$  the entire loops coincide in phase space and the local oscillation is effectively period-1.

#### IV REPRESENTATION OF LOOP EXCHANGES AS BRAID MOVES

Synchronization defect lines are associated with loop exchanges; thus, the topological analysis of loop exchanges provides a framework to classify the types of defect lines. Here we shall sketch the connection between loop exchanges and operations on closed braids for period-2 dynamics; generalization to period- $n$  provides a classification of all line defect types [4].

Since the phase jump on the  $\Omega$  curve is an integer multiple of  $2\pi$  a coarse grained description of an orbit may be constructed in the following way: suppose that at  $t = t_0$  the phase point of the period- $n$  orbit is on the  $m_1$ -th loop and at  $t = t_0 + T_n/n$  on the  $m_2$ -th loop, etc., until at  $t = t_0 + T_n$  the phase point returns to the  $m_1$ -th loop and the pattern  $(m_1, m_2, \dots, m_n)$  repeats. Here  $m_l \in [1, n]$ ,  $l \in [1, n]$ ,  $m \neq l$ . The symbolic string  $s = (m_1, \dots, m_n)$  constitutes a coarse-grained representation of the orbit. For example, for period 2 we have only two symbolic strings,  $s_1 = (12)$  and  $s_2 = (21)$ . In this representation an oscillation shifted by  $2\pi$  forward relative to  $s$  is given by  $(m_2, \dots, m_n, m_1)$  while an oscillation shifted by  $2\pi$  backward is  $(m_n, m_1, \dots, m_{n-1})$ . Any phase translation by  $\pm 2\pi k$  corresponds to one of the  $n$  cyclic permutations of the symbolic string  $s$ .

From this discussion we see that loop exchanges may be represented symbolically by permutations which take a loop  $m_i$ ,  $i = 1, \dots, n$  of a period- $n$  orbit to another loop  $m_j$ ,  $j = 1, \dots, n$ ,  $j \neq i$  of the same orbit. For example, when the  $\Omega$  curve in a period-2 system is crossed loops 1 and 2 of the orbit exchange; this exchange is may be represented by the permutation  $\begin{pmatrix} 12 \\ 21 \end{pmatrix}$  acting on the string  $s_1 = (12)$ ,

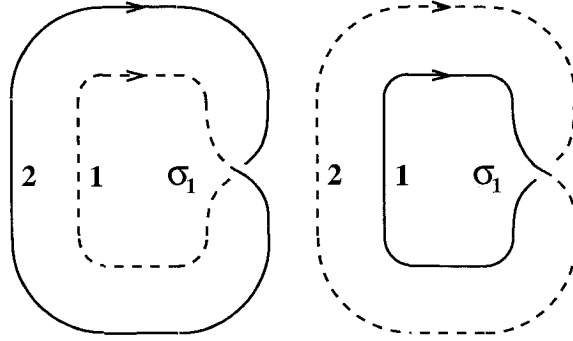


**FIGURE 5.** Schematic representation of the projection of a period-2 orbit as a closed braid. The braid in the right panel is obtained from that in the left panel by propagation of  $\sigma_1$  around  $\overline{B_2}$ .

$$\begin{pmatrix} 12 \\ 21 \end{pmatrix} (12) = (21) = s_2. \quad (7)$$

A schematic representation of a period-2 orbit projected onto a two-dimensional phase plane is shown in Fig. 5 (left panel). Topologically this is a closed braid denoted  $\overline{B_2}$  composed of the open elementary braid  $\sigma_1$  and the parallel threads that close it [12]. The designation  $\sigma_i$  is used if thread  $i$  overcrosses thread  $i + 1$  while  $\sigma_i^{-1}$  corresponds to undercrossing. Examination of Fig. 5 shows that if the crossing is moved counterclockwise (opposite to the direction of the flow indicated by the arrows) around the braid in the left panel one arrives at the braid in the right panel where the loops have interchanged. Technically this operation is the first Markov move  $\mathcal{M}_1^{(1)}$ . The exchange of loops induced by  $\mathcal{M}_1^{(1)}$  can be described by the exchange operator  $\mathcal{A}_1^{(1)}$  represented by the permutation  $\begin{pmatrix} 12 \\ 21 \end{pmatrix}$ . Since a period-2 oscillation has only two strings  $s_1 = (12)$  and  $s_2 = (21)$ , action of  $\mathcal{A}_1^{(1)}$  on one of them gives the other and vice-versa

$$\begin{aligned} \mathcal{A}_1^{(1)} s_1 &= \begin{pmatrix} 12 \\ 21 \end{pmatrix} (12) = (21) = s_2, \\ \mathcal{A}_1^{(1)} s_2 &= \begin{pmatrix} 12 \\ 21 \end{pmatrix} (21) = (12) = s_1. \end{aligned} \quad (8)$$

The action of  $\mathcal{A}_1^{(1)}$  is equivalent to a translation of the oscillation by half a period or a  $2\pi$  phase shift for period 2. One may return to the original configuration by application of the reverse move  $(\mathcal{M}_1^{(1)})^{-1}$  which propagates  $\sigma_1$  along the flow or apply  $\mathcal{M}_1^{(1)}$  again. Thus, the inverse operator  $(\mathcal{A}_1^{(1)})^{-1}$  induced by  $(\mathcal{M}_1^{(1)})^{-1}$  is equivalent to  $\mathcal{A}_1^{(1)}$ . The operator  $\mathcal{A}_1^{(1)}$  generates a group

$$(\mathcal{A}_1^{(1)})^{-1} = \mathcal{A}_1^{(1)}, \quad (\mathcal{A}_1^{(1)})^{-2} = (\mathcal{A}_1^{(1)})^2 = \hat{\mathbf{1}}. \quad (9)$$



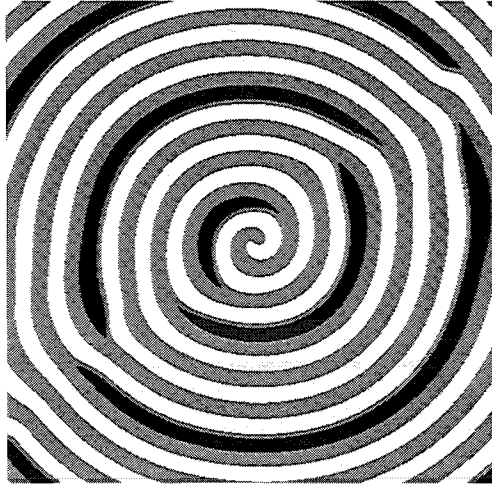


**FIGURE 7.** Period-3 spiral wave with two synchronization line defects in the excitable medium described by Eq. (10). The concentration field  $v(\mathbf{r})$  is color-coded as shown in Fig. 6.

$$\begin{aligned}\frac{\partial u}{\partial t} &= \frac{1}{\varepsilon}u(1-u)\left(u - \frac{v+b}{a} - f(v)\right) + D\nabla^2 u, \\ \frac{\partial v}{\partial t} &= u - v,\end{aligned}\tag{10}$$

with

$$f(v) = \alpha \exp\left(-\frac{(v-v_0)^2}{\sigma^2}\right).$$

If the system is displaced from the stable fixed point  $u = 0, v = 0$  to the right of the unstable branch of the nullcline  $\dot{u} = 0$  it rapidly evolves to the upper stable branch  $u = 1$  which it follows until  $v$  reaches sufficiently large values. It then jumps to the lower stable branch  $u = 0$  and slowly relaxes to the steady state. The unstable branch of the nullcline  $\dot{u} = 0$  nearly touches the nullcline  $\dot{v} = 0$  (see Fig. 6). Consequently, if another excitation is applied before the system has reached the stationary state it may execute a second, smaller excitable loop before it finally attains the stable state. Figure 7 shows period-3 spiral wave with two synchronization line defects. The entire concentration field slowly rotates with constant angular velocity  $\omega$  about the spiral core. In a coordinate frame rotating with angular velocity  $\omega$  it takes three rotations of the spiral for the concentration field to return into itself. For period-3 complex-excitable dynamics with total phase increment of  $6\pi$  one might expect to find one line defect with a  $4\pi$  jump or two lines, each with a  $2\pi$  jump. In Fig. 7 the two defect lines which emanate from the spiral core are associated with  $2\pi$  phase jumps arising from the loop exchange process described earlier for complex-oscillatory media.

## VI LINE DEFECT DYNAMICS AND TURBULENCE

We now describe how  $\Omega$  lines organize the medium and discuss the factors that govern their movement. Before doing so it is useful to represent the concentration field in a form that highlights the line defects. Suppose the spiral wave system is in the period-4 regime and during four spiral rotations the  $c_z(\mathbf{r})$  concentration maxima  $A_i(\mathbf{r}), i = \overline{1,4}$  are monitored at every point in the medium and sorted so that  $A_1(\mathbf{r}) \leq A_2(\mathbf{r}) \leq A_3(\mathbf{r}) \leq A_4(\mathbf{r})$ . The scalar fields  $\xi_1(\mathbf{r}) = A_4(\mathbf{r}) - A_1(\mathbf{r})$  and  $\xi_2(\mathbf{r}) = A_4(\mathbf{r}) - A_3(\mathbf{r})$  can be used to characterize the  $\Omega$  lines since they take on fixed, non-zero values at points in the medium with period-4 dynamics and vanish at points where loop exchanges occur. In fact,  $\xi_1(\mathbf{r})$  is zero on  $\Omega_1$  curves while  $\xi_2(\mathbf{r})$  vanishes on both  $\Omega_1$  and  $\Omega_2$  curves. Figure 8, panel (c), shows  $\xi_2(\mathbf{r})$  for a spiral pair in a system with periodic boundary conditions. The  $\varphi(\mathbf{r}, t_0)$  and  $c_z(\mathbf{r}, t_0)$  fields are shown in panels (a) and (b), respectively, for the same value of  $C = 4.30$ . The cores of spiral waves are connected by an  $\Omega_1$  curve (wide, nearly straight black line). The dynamics in the bulk of the medium is period-4. The shock lines where the spiral waves collide are seen in panels (c) and (d) as one vertical and two horizontal strips

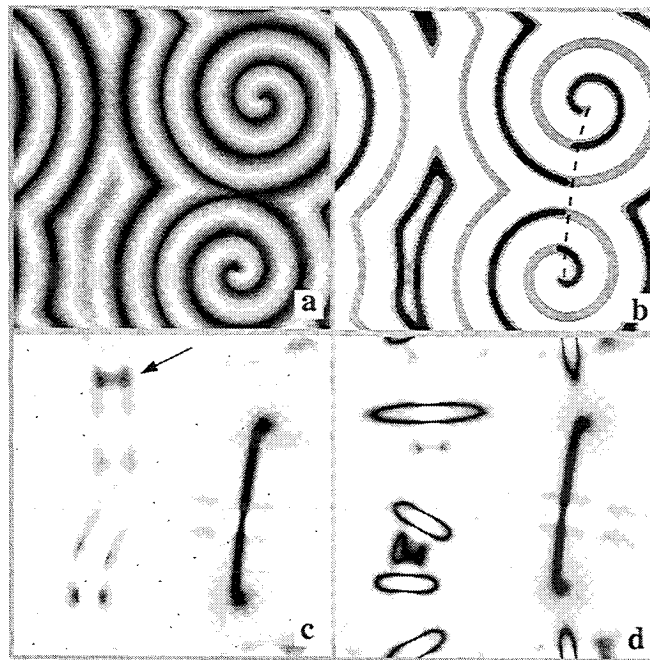


**FIGURE 8.** Representation of defect lines by the  $\xi_2(\mathbf{r})$  field for the medium with two spiral waves at  $C = 4.30$  (c) and  $C = 4.32$  (d). Panels (a) and (b) show, respectively, the  $\varphi(\mathbf{r}, t_0)$  and  $c_z(\mathbf{r}, t_0)$  fields calculated for the medium in panel (c).

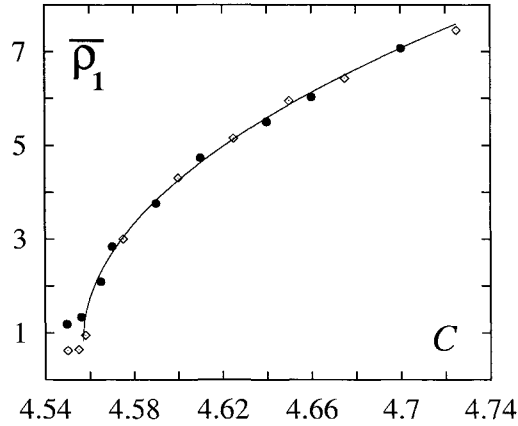


**FIGURE 9.** Transition to  $\Omega_1$ -line turbulence; diamonds, system with two spirals shown in Fig. 8; filled circles, system of the same size with four spirals.

where the grey shades are inhomogeneous indicating that the local dynamics on the shock lines is different from that in the bulk. An analysis of the local trajectories shows that the dynamics smoothly transforms from periodic to chaotic as one enters the shock region. The chaotic dynamics on the shock lines induces fluctuations of the  $A_i(\mathbf{r})$  fields seen in Fig. 8(c) as dark spots. Sufficiently large fluctuations may produce bubble domains delineated by closed  $\Omega_2$  curves (cf. Fig. 8(d)). As one progresses in parameter space towards chaos, the bubble nuclei begin to proliferate forming large domains whose growth is controlled by collisions with spiral cores or other domains [6].

Two factors are primarily responsible for the dynamics of the  $\Omega$  lines: diffusion tends to reduce the curvature of the lines and leads to their shrinkage, while the phase gradient gives rise to propagation to the spiral cores and leads to their growth. One may in fact verify that these two factors are sufficient to predict the critical size of a line defect bubble [6]. If the system parameters are tuned beyond a critical value, supercritical nuclei of bubbles formed on the shock lines grow to fill the system. Their density saturates at a finite value due to a balance between collisions of defect lines which reduce their total length and the nucleation process which generates new line defects. This type of line defect turbulence is signalled by the growth of the order parameters  $\rho_1$  or  $\rho_2$ , the densities of the  $\Omega_1$  or  $\Omega_2$  defect lines. The growth of  $\rho_1$  for  $\Omega_1$  line turbulence is shown in Fig. 9. Both the  $\rho_1$  and  $\rho_2$  order parameters show power law growth with the distance from the critical value,

$$\bar{\rho}_i(C) \sim (C - C_{\Omega_i})^{\alpha_i}, \quad (11)$$

with  $(C_{\Omega_2} = 4.306, \alpha_2 = 0.249 \pm 0.006)$  and  $(C_{\Omega_1} = 4.557, \alpha_1 = 0.491 \pm 0.005)$ ,

respectively, indicating that these transitions to turbulence have the character of non-equilibrium phase transitions.

## VII CONCLUSION

When the local dynamics is more complex than simple periodic motion the possibility of distinctive types of pattern formation arises. We have described how synchronization defect lines may arise in spiral wave systems and discussed their types and properties. As such systems are tuned to lie closer to chaotic regimes the line defects may nucleate at shock zones in the medium where wave fronts collide. The growth of line defects as a result of phase-gradient-driven motion in the system in competition with the tendency of diffusion to reduce the line curvature and length determines the critical nucleus size. Turbulent regimes are characterized by growth of defect line and their destruction through collisions.

Line defects may be found in systems without spiral waves. However, if the system is sufficiently homogeneous that phase gradients are small line defects may be produced in nucleation events but they will always shrink. It is also possible to prepare line defects in target pattern states where no spiral waves exist.

As one progresses deep into chaotic regimes the line defects are destroyed and amplitude turbulence ensues. However, it is still possible to have phase synchronized chaotic states in this case and spiral waves can be sustained in such chaotic media.

The work presented here suggests that a variety of unexplored phenomena exist in spatially distributed media with complex-periodic or chaotic dynamics. In addition to the observations of defect lines in the laboratory experiments mentioned above, one might expect to find them in natural systems exhibiting complex-periodic dynamics.

## REFERENCES

1. M. Rosenblum, A. Pikovsky, and J. Kurths, *Phys. Rev. Lett.* **76**, 1804 (1996); G. Osipov, A. Pikovsky, M. Rosenblum, and J. Kurths, *Phys. Rev. E* **55**, 2357 (1997).
2. R. Klevecz, J. Pilliod, and J. Bolen, *Chronobiology International* **8**, 6 (1991).
3. L. Brunnet, H. Chaté, and P. Manneville, *Physica D* **78**, 141 (1994).
4. A. Goryachev and R. Kapral, *Phys. Rev. Lett.* **76**, 1619 (1996); A. Goryachev and R. Kapral, *Phys. Rev. E* **54**, 5469 (1996).
5. A. Goryachev, H. Chaté, and R. Kapral, *Phys. Rev. Lett.* **80**, 873 (1998).
6. A. Goryachev, H. Chaté, and R. Kapral, "Transitions to Line Defect Turbulence in Complex-Oscillatory Media", *Phys. Rev. Lett.*, in press, 1999.
7. J.-S. Park, and K. Lee, "Complex Periodic Spirals and Line-Defect Turbulence in a Chemical System", preprint, 1999.
8. M. Yoneyama, A. Fujii, and S. Maeda, *J. Am. Chem. Soc.* **117**, 8188 (1995).
9. N. D. Mermin, *Rev. Mod. Phys.* **51**, 591 (1979).

10. P. S. Hagan, *SIAM J. Appl. Math.* **42**, 762 (1982).
11. O. E. Rössler, *Z. Naturforsch.* **31**, 1664 (1976).
12. J. S. Birman, *Braids, Links and Mapping Class Groups*, Princeton Univ. Press, Princeton, 1974.
13. A. Giaquinta, S. Boccaletti, L. Tellini, and F. Arrecchi, *CHAOS* **4**, 557 (1994).
14. A. Goryachev, and R. Kapral, to appear in *Int. J. Bifurcation and Chaos* (1999).